Supplemental Document

Stress amplification during development of the tendon-to-bone attachment

Yanxin Liu, Annie Gitomer Schwartz, Victor Birman,
Stavros Thomopoulos, Guy M. Genin

1 Material properties of mineralized collagen tissue

Our morphometrical data of supraspinatus tendon-to-bone insertion site development in a developing mouse model showed that there existed an approximately linear increase of mineral content in the collagen matrix throughout post-natal development. The partially mineralized tissue at the insertion site was assumed to be transversely isotropic (i.e., similar to tendon). In a recent study (Liu 2012), we developed models to predict the longitudinal and transverse moduli of mineralized collagen tissue with respect to mineral volume fraction, based on the nanoscale details of the accumulation of mineral onto/into collagen fibrils. The results obtained from finite element analysis, assuming that mineral platelets first filled up the gap channels of collagen fibrils, and that the further mineralization proceeded with random accumulation of extrafibrillar mineral are shown in Fig. S1.

The maximum volume fraction of mineral was estimated to be about 0.41 with no presence of intrafibrillar mineralization in the overlap regions of collagen fibrils, based on the steric model developed by Alexander et al. (2012). Without mineralization, the moduli of the tendon are $E_1 = 480$ MPa, $E_2 = 2.28$ MPa; with full mineralization, $E_1 = 1.31E_{bone}$, $E_2 = 0.84E_{bone}$, where $E_{bone} = 20$ GPa. The Poisson's ratio ν_{23} in the transversely plane was assumed to be 0.3, Poisson's ratio ν_{12} was assumed to be 0.1 at all points, which satisfied the positive definitive constraint of the stiffness tensor. Shear modulus $G_{12} = 3\beta E_1 (R/L)^2$, where $\beta = 1.07$, aspect ratio of collagen fibers $(R/L) = 1:20$ (Genin et al. 2009).

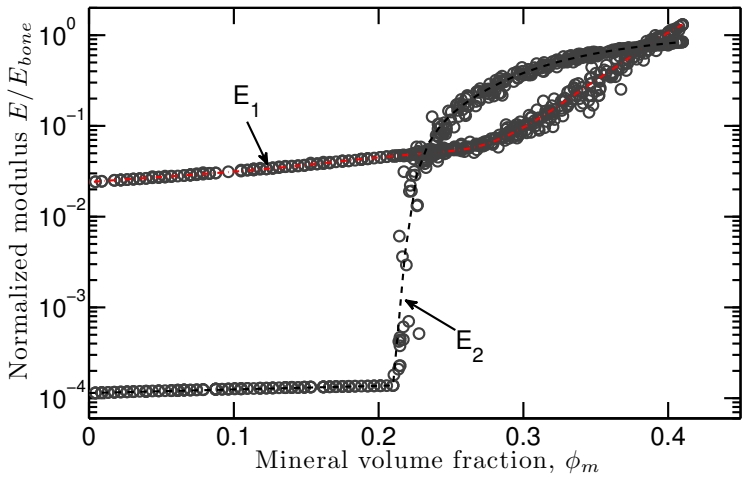

Fig. S1: Moduli of extrafibrillar matrix in the mineralized region at the insertion site, normalized with respect to $E_{bone} = 20$ GPa.

2 Stress analysis of concentric ring model

The details of the stress analysis of a concentric ring model loaded with uniform tensile stress $\sigma_r = p$ at the outermost boundary is presented by Liu et al. (2012). We show the principal equations here that were employed in the calculation of the global stress concentration factor in the current paper.

The stress field was obtained by neglecting out-of-plane stresses, and assuming small deformations. The bone core was assumed isotropic and the bands modeling the insertion site and tendon were transversely isotropic (M transversely isotropic bands in total for tendon and insertion site). The bands were perfectly bonded, with the outer radius of the m^{th} band denoted by R_m. The in-plane mechanical properties of the m^{th} band included three constants: the elastic moduli in the radial and tangential directions, $E_r^{(m)}$ and $E_\theta^{(m)}$, respectively, and the Poisson's ratio $\nu_{r\theta}^{(m)}$ that indicates the degree of tangential contraction associated

with radial stretching. The other Poisson's ratio depends upon the specified above material constants of the ring: $\nu_{\theta r}^{(m)} = \nu_{r\theta}^{(m)} E_\theta^{(m)} / E_r^{(m)}$.

The radial and tangential stresses in the m^{th} orthotropic ring due to radial compressive stresses q_m and q_{m+1} applied at the outer and inner interfaces of the m^{th} band, respectively, are:

$$\begin{aligned}
\sigma_r^{(m)}(r) = {} & \frac{q_{m-1} c_m^{k_m+1}}{1-c_m^{2k_m}} \left[\left(\frac{r}{R_m} \right)^{k_m-1} - \left(\frac{R_m}{r} \right)^{k_m+1} \right] \\
& + \frac{q_m}{1-c_m^{2k_m}} \left[-\left(\frac{r}{R_m} \right)^{k_m-1} + c_m^{2k_m} \left(\frac{R_m}{r} \right)^{k_m+1} \right] \\
\sigma_\theta^{(m)}(r) = {} & \frac{q_{m-1} c_m^{k_m+1}}{1-c_m^{2k_m}} k_m \left[\left(\frac{r}{R_m} \right)^{k_m-1} + \left(\frac{R_m}{r} \right)^{k_m+1} \right] \\
& - \frac{q_m}{1-c_m^{2k_m}} k_m \left[\left(-\frac{r}{R_m} \right)^{k_m-1} + c_m^{2k_m} \left(\frac{R_m}{r} \right)^{k_m+1} \right]
\end{aligned} \tag{S1}$$

where r is the radial coordinate measured from the center of the bone, $c_m = R_{m-1}/R_m$, and $k_m = \sqrt{E_\theta^{(m)}/E_r^{(m)}}$. The stress field in the isotropic bone depends only on the stress at its outer boundary, $\sigma_r = \sigma_\theta = -q_0$. The continuity requirement for radial displacements along the boundaries of the adjacent bands, $u_r^{(m)}(r = R_m) = u_r^{(m+1)}(r = R_m), m = 1, 2, ..., M$ and along the bone-to-insertion boundary $u_r^{(0)}(r = R_0) = u_r^{(1)}(r = R_0)$ yields M equations for the M unknown values of q_m:

$$\begin{aligned}
q_0 = 2 q_1 k_1 c_1^{k_1-1} & \left(\frac{E_\theta^{(1)}}{E_{bone}} (1-\nu_{bone})(1-c_1^{2k_1}) + \left[(1+c_1^{2k_1}) k_1 + (1-c_1^{2k_1}) \nu_{\theta r}^{(1)} \right] \right)^{-1} \\
0 &= q_0 R_0 \alpha_1 + q_1 R_1 \beta_1 + q_2 R_2 \alpha_2 \\
0 &= q_1 R_1 \alpha_2 + q_2 R_2 \beta_2 + q_3 R_3 \alpha_3 \\
& \vdots \\
0 &= q_{M-2} R_{M-2} \alpha_{M-1} + q_{M-1} R_{M-1} \beta_{M-1} + \sigma_M R_M \alpha_M
\end{aligned} \tag{S2}$$

where $\sigma_M = -p$ is the inward radial stress applied to the outer boundary of the outermost band representing the tendon, and

$$\begin{aligned}
\alpha_m &= \frac{2 k_m c_m^{k_m}}{E_\theta^{(m)} (1-c_m^{2k_m})} \\
\beta_m &= \frac{1}{E_\theta^{(m)}} \left[\nu_{\theta r}^{(m)} - k_m \frac{(1+c_m^{2k_m})}{(1-c_m^{2k_m})} \right] - \frac{1}{E_\theta^{(m+1)}} \left[\nu_{\theta r}^{(m+1)} + k_{m+1} \frac{(1+c_m^{2k_{m+1}})}{(1-c_m^{2k_{m+1}})} \right]
\end{aligned} \tag{S3}$$

3 Homogenized moduli of mineralized and unmineralized regions at the insertion site during development

The homogenized longitudinal (E_1) and transverse (E_2) moduli for the mineralized fibrocartilage (MF) and unmineralized fibrocartilage (UF) during development are listed in Table S1. The superscripts *ub*, *avg* and *lb* correspond to the upper bound, average value, and lower bound of volume fraction of cells in the corresponding region.

Table S1: Homogenized moduli calculated from the axisymmetrical unit cell model for the mineralized and unmineralized regions at the insertion site as functions of the development time. Note that although at most two digits are significant, extra digits are included because rounding would cause some moduli to exceed thermodynamic limits

modulus (MPa)	7d	10d	14d	28d	56d
$(E_1^{ub})_{MF}$	128.2	204.2	345.5	619.3	698.5
$(E_1^{avg})_{MF}$	184.5	238.4	497.6	667.5	719.0
$(E_1^{lb})_{MF}$	242.2	273.3	678.4	719.6	740.3
$(E_2^{ub})_{MF}$	1813	2135	2706	3623	3821
$(E_2^{avg})_{MF}$	2052	2278	3254	3748	3865
$(E_2^{lb})_{MF}$	2293	2421	3774	3867	3909
$(E_1^{ub})_{UF}$	176.1	251.3	216.8	308.8	290.2
$(E_1^{avg})_{UF}$	200.3	252.6	272.6	324.0	310.3
$(E_1^{lb})_{UF}$	225.6	253.9	337.6	340.0	331.7
$(E_2^{ub})_{UF}$	1.252	1.606	1.444	1.866	1.784
$(E_2^{avg})_{UF}$	1.366	1.612	1.704	1.932	1.873
$(E_2^{lb})_{UF}$	1.486	1.618	1.989	1.999	1.964

References

Alexander B, Daulton TL, Genin GM, Lipner J, Pasteris JD, Wopenka B, Thomopoulos S (2012) The nanometre-scale physiology of bone: steric modelling and scanning transmission electron microscopy of collagen–mineral structure. J R Soc Interface

Genin GM, Kent A, Birman V, Wopenka B, Pasteris JD, Marquez PJ, Thomopoulos S (2009) Functional grading of mineral and collagen in the attachment of tendon to bone. Biophys J 97(4):976–985

Liu YX (2012) The mechanics of bimaterial attachment at the tendon-to-bone insertion site. PhD thesis, Washington University in St. Louis

Liu YX, Thomopoulos S, Birman V, Li JS, Genin GM (2012) Bi-material attachment through a compliant interfacial system at the tendon-to-bone insertion site. Mech Mater 44:83–92